Foaming of poly(3-hydroxybutyrate-co-3-hydroxyvalerate)/organo-clays nano-biocomposites by a continuous supercritical CO2 assisted extrusion process

Nicolas Le Moigne, Martial Sauceau, Mohamed Benyakhlef, Rabeb Jemai, Jean-Charles Bénézet, Élisabeth Rodier, José-Marie Lopez-Cuesta, Jacques Fages

▶ **To cite this version:**

Nicolas Le Moigne, Martial Sauceau, Mohamed Benyakhlef, Rabeb Jemai, Jean-Charles Bénézet, et al.. Foaming of poly(3-hydroxybutyrate-co-3-hydroxyvalerate)/organo-clays nano-biocomposites by a continuous supercritical CO2 assisted extrusion process. European Polymer Journal, 2014, 61, pp.157-171. 10.1016/j.eurpolymj.2014.10.008 . hal-01611610

HAL Id: hal-01611610
https://hal.science/hal-01611610

Submitted on 6 Nov 2017

HAL is a multi-disciplinary open access archive for the deposit and dissemination of scientific research documents, whether they are published or not. The documents may come from teaching and research institutions in France or abroad, or from public or private research centers.

L'archive ouverte pluridisciplinaire **HAL**, est destinée au dépôt et à la diffusion de documents scientifiques de niveau recherche, publiés ou non, émanant des établissements d'enseignement et de recherche français ou étrangers, des laboratoires publics ou privés.

Foaming of poly(3-hydroxybutyrate-co-3-hydroxyvalerate)/organo-clays nano-biocomposites by a continuous supercritical CO_2 assisted extrusion process

Nicolas Le Moigne [a,*], Martial Sauceau [b,*], Mohamed Benyakhlef [a], Rabeb Jemai [b], Jean-Charles Benezet [a], Elisabeth Rodier [b], José-Marie Lopez-Cuesta [a], Jacques Fages [b]

[a] *Centre des Matériaux des Mines d'Alès (C2MA), Ecole des Mines d'Alès, 6 avenue de Clavières, F-30319 Alès, France*[1]
[b] *Université de Toulouse, Ecole des Mines d'Albi, CNRS, Centre RAPSODEE, F-81013 Albi, France*

A B S T R A C T

A continuous supercritical carbon dioxide (sc CO_2) assisted extrusion process has been used to prepare poly(3 hydroxybutyrate co 3 hydroxyvalerate) PHBV/organo clays nano biocomposite foams by two methods: a one step method based on the direct foaming of physical PHBV/clays mixtures, and a two step method based on the foaming of extruded PHBV/clays mixtures prepared beforehand by twin screw extrusion. The structures obtained have been characterized in terms of clay dispersion, matrix crystallization, poros ity and pore size distribution and pore density. The influence of processing conditions as temperature, pressure, CO_2 mass fraction and the clays/foaming interrelationships have been elucidated. It was shown that the prior preparation of a masterbatch by twin screw extrusion and its dilution during the foaming process is a necessary step to improve clay dispersion without extensive thermal degradation of PHBV. By controlling the sc CO_2 mass fraction in a narrow window, good clay dispersion appears to favour homogeneous nucleation while limiting the coalescence of the pores, and hence allowed to obtain nano biocomposite foams with better homogeneity and higher porosity up to 50%.

1. Introduction

Bio based polymers like polyhydroxyalkanoates (PHAs) are marketed as eco friendly alternatives to the currently widespread non degradable oil based thermoplastics, due to their natural and renewable origin, their biodegradabil ity and biocompatibility. PHAs are biopolyesters made of different types and amounts of HAs. They are synthesized by microorganisms from various carbon sources as an intracellular carbon and energy stock. Poly 3 hydroxybuty rate (PHB) was the first member of this bio based polymer group to be discovered, and has been the most widely studied PHA [1]. Its properties are similar to various syn thetic thermoplastics like polypropylene and hence it can be used alternatively in several applications, especially for agriculture, packaging but also biomedicine where bio degradability and biocompatibility are at stake. However, some drawbacks have prevented its introduction to the market as an effective alternative to the oil based thermo plastics. In particular, PHB is indeed brittle and presents a slow crystallization rate and a poor thermal stability, which makes it difficult to process [2 5].

* Corresponding authors. Tel.: +33 (0)4 66 78 53 02; fax: +33 (0)4 66 78 53 65 (N. Le Moigne). Tel.: +33 5 63 49 33 18; fax: +33 5 63 49 30 25 (M. Sauceau).

E-mail addresses: Nicolas.Le Moigne@mines ales.fr (N. Le Moigne), Martial.Sauceau@mines albi.fr (M. Sauceau).

[1] C2MA is member of the European Polysaccharide Network of Excel lence (EPNOE), www.epnoe.eu.

In order to control the PHB properties, several kinds of PHAs copolymers have been described in the literature such as the poly(3 hydroxybutyrate co 3 hydroxyvaler ate) (PHBV) with various hydroxyvalerate (HV) contents and molecular weights, which present better mechanical properties, lower melting temperature and an extended processing window [6]. Improved properties can be also obtained by the addition of nanoparticles such as clays. Indeed, clay minerals present high aspect ratio and specific surface, and can be dispersed in small amounts in polymer matrices to prepare nanocomposites with improved ther mal stability, mechanical properties or barrier properties [7]. Several studies have been achieved on the preparation and the characterization of PHBV/clay systems. One of the key parameters is the quality of the clay dispersion that can be controlled by the elaboration route either the sol vent intercalation, the *in situ* intercalation or the melt intercalation; the latter being preferred for a sustainable development since it limits the use of organic solvents [2]. The melt intercalation route is usually achieved by twin screw extrusion and the processing conditions are of great importance. The screw profile, the feed rate, the screw speed, the operating temperatures as well as the mixing sequences, i.e. direct mixing or dilution of master batches, influence greatly the quality of the clay dispersion [8,9]. The organomodifiers inserted in clays interlayer spaces to improve polymer/clay affinity and the polymer chains intercalation have a strong influence on the disper sion but also to catalyse the PHBV degradation during pro cessing [6,10].

The use of supercritical fluids has recently appeared as an innovative way to improve clay dispersion leading to new "clean and environment friendly" processes. Supercrit ical carbon dioxide (sc CO_2) is often used because it is non toxic, non flammable, chemically inert, and its supercritical conditions are easily reached [11]. Sc CO_2 has also more favourable interaction with polymers compared to other inert gases and it has the ability to dissolve in large quanti ties and to act as a plasticizer, which modify drastically polymer properties (viscosity, interfacial tension, etc.). In addition, the dissolved sc CO_2 can act as a foaming agent during processing [12]. It is therefore possible to master pore generation and growth by controlling the operating conditions [13], and to generate low density porous struc tures of interest for lighter packaging or as carriers of active ingredients, e.g. for drug release applications. PHB and its copolymers have already exhibited good compatibility with sc CO_2. The solubility of PHB in supercritical carbon dioxide can reach several g/L [14] and a high sorption degree can be achieved [15]. Moreover, the authors have shown that an increase from 8% to 12% of the HV content in the copolymer results in an increase in the sorption degree because HV blocks induce higher molecular mobility.

All these features make sc CO_2 also able to modify the nanoparticles dispersion inside polymer matrices, which in turn has an effect on the foam structure. Improved disper sion of clays and modified porous structures have been obtained with sc CO_2, mainly in batch processes via the *in situ* intercalation method, with various nanocomposite systems such as polydimethysiloxane (PDMS)/clays [16], polystyrene (PS)/clays [17] and recently polylactic acid (PLA)/clays [18]. As an alternative to batch processes, con tinuous processes such as sc CO_2 assisted extrusion or injec tion are very promising since they are more easily adaptable for an industrial scale up. Incorporating sc CO_2 in continu ous processes is also of great interest because its plasticiza tion capacity decreases the viscosity of molten polymers and allows to limit the mechanical stresses and the operat ing temperatures during processing [13]. This is particularly interesting for polymers having a limited thermal stability as biopolyester. For instance, it has been shown that the melting temperature of PHB and PHBV decrease respec tively from 178 to 151 °C and from 171 to 137 °C for pres sures up to 35 MPa [19]. In the same work, melt processing of PHB and PHBV, which are prone to thermal degradation upon melting in ambient atmosphere, was achievable without degradation in CO_2 medium. The inter actions with other polymers could also been modified by the presence of sc CO_2. Jenkins et al. [20] have studied the PHBV PCL blend system by the use of mechanical blending in the presence of supercritical CO_2. They showed that PHBV PCL blends produced by mechanical means were immiscible and degraded, whereas the same blends produced using supercritical methods were found to be mis cible over the lower wt% PHBV compositions and less degraded.

Recently, efforts have been made to produce high expanded PLA foams from sc CO_2 assisted extrusion [21 24]. A growing number of studies also reported on the preparation of nanocomposites systems with clays nano particles by sc CO_2 assisted continuous processes. Differ ent processing methods were used e.g. two step extrusion process [25 27], sc CO_2 assisted single screw extrusion [28], single screw extrusion with prior prepara tion of exfoliated nanocomposites by *in situ* polymeriza tion [29] or the injection of sc CO_2/clays mixtures in the extruder [30]. In most cases, the authors obtained an increased cell density, a smaller cell size and improved performances with exfoliated nanocomposite foams. More recently, the effect of nanoclay on the foamability of PLA was investigated [31,32]. The results showed that both the cell density and the expansion ratio were greatly pro moted with increased clay content. Zhao et al. [33,34] have investigated the possibility to use a supercritical nitrogen (sc N_2) assisted injection molding process to develop microcellular PLA/PHBV clay nanocomposites. The results showed a decrease of the average cell size and an increased cell density with the addition of clays in PLA/PHBV blends. Rheological behaviour of the PLA/PHBV/clays nanocompos ites suggests a good dispersion of the clays within the matrix. Javadi et al. [35] have also used sc N_2 to foam PHBV poly (butylene adipate co terephthalate) (PBAT) hyperbranched polymer (HBP) nanoclay (NC). Microcellu lar nanocomposites exhibited a mixture of exfoliated and intercalated structures. Moreover, dispersed clays improved the thermal stability, reduced the cell size and increased the cell density of the foams.

Structuring bio based polymers such as PHAs by effi cient and environmental friendly processes thus appears as a key issue towards new applications. Of particular inter est are supercritical CO_2 assisted processes, which are able to modify the behaviour of polymeric materials from the

macromolecular level (plasticization, crystallization kinetics) to the microstructural level (generation of porous structures through nucleation/growth phenomena). In this study, we have developed a continuous supercritical CO_2 assisted extrusion process to foam PHBV/clay nano biocomposites, and the effects of clays and processing routes and conditions on foam structures are investigated. The dispersion of the clays and the foaming of the PHBV matrix were achieved by two processing methods: a one step method based on the direct foaming of physical PHBV/clays mixtures, and a two step method based on the foaming of PHBV/clays mixtures prepared beforehand by twin screw extrusion. At first, the structure and rheological behaviour of PHBV/clays extruded mixtures prepared by twin screw extrusion are characterized. These results are then used to produce and compare nano biocomposite foams based on the two processing methods of clay incorporation. The resulting structures are characterized and the influence of the operating conditions and the clays/foaming interrelationships are discussed.

2. Materials and methods

2.1. Materials

PHBV produced by bacterial fermentation with a HV content of 13% w/w, nucleated and plasticized with 10% of a copolyester was purchased from Biomer (Germany). It is a semi crystalline polymer with a glass transition temperature of 5 °C and a melting temperature with two peaks at 153 and 162 °C. The weight average molecular weight is Mw = 600 kDa. The clay used is a Cloisite C30B (C30B) produced by Southern Clay Products, Inc. (USA). It is a montmorillonite (MMT) organo modified by a quaternary ammonium salt, i.e. tallow alkyl bis(2 hydroxyethyl) methylammonium chloride, with a cation exchange capacity of 90 meq/100 g. The tallow alkyl is a mixture that contains 65% of C18, 30% of C16, and 5% of C14 alkyl chains. C30B presents a moisture content <3% and a weight loss on ignition of 30%. To limit hydrolysis of PHBV upon processing, C30B and PHBV were dried before use at 80 °C overnight and 4 h, respectively.

2.2. Preparation of PHBV/C30B extruded mixtures (EX)

PHBV based nanocomposites containing 2.5% w/w C30B, noted PHBV/2.5% C30B (EX), and PHBV based masterbatches containing 10%, 20% w/w C30B, noted PHBV/10% and 20% C30B (EX), were prepared by melt intercalation using a co rotating twin screw extruder BC21 (Clextral, France) having a length of 1200 mm, a screw diameter of 25 mm and a L/D (length to diameter ratio) of 48. The twin screw profile used is presented in Fig. 1.

As shown in Fig. 1, a parabolic temperature profile was used to limit thermal degradation of PHBV taking into account the HV content [36 38]. C30B clays were introduced in zone 4, the overall feed rate was 4 kg/h and the screw speed was 250 rpm. The mixing and the dispersion of the C30B clays within the PHBV matrix are ensured by two kneading sections with stagger angles between the kneading paddles of 45° and 90° in zones 6 and 9, respectively. Extrudates were water cooled at ambient temperature, then pelletized in line to 3 mm diameter and dried overnight at 50 °C under vacuum (10 kPa). About 2.5 kg of granules were collected for each batch. For comparison, pure PHBV was also processed and analyzed in the same conditions.

All the batches were also moulded by injection with a Krauss Maffei KM 50 180 CX into test specimens. The barrel to die temperature profile was 40 165 °C with a screw speed of 50 rpm. Samples were maintained at 12 MPa then cooled down during 30 s at 25 °C. PHBV based masterbatches containing 10%, 20% w/w C30B were diluted to 2.5% w/w C30B, noted PHBV/2.5% C30B dil. 10% and 20% (EX), in the injection molding machine to analyze the effect of the dilution on the nanocomposite structures and properties. As will be shown in the following, the composites from the dilution of the 20% w/w C30B masterbatch to 2.5% w/w C30B, gave similar clay dispersion and limited thermal degradation as compared to the PHBV based nanocomposites containing 2.5% w/w C30B. This dilution procedure was thus used to produce nanocomposite foams by sc CO_2 assisted extrusion.

2.3. Preparation of PHBV/C30B physical mixtures (PM)

In addition to extruded mixtures, physical mixtures of PHBV pellets with 2.5% w/w of C30B, noted PHBV/2.5% C30B (PM), were prepared with a simple manual batch mixing. Fig. 2a shows the kinetics of triboelectrification of PHBV and C30B as a function of rotation time measured by placing a mixture of both components in a stainless steel rotative drum for 10 min (Faraday cage linked to Keithley 6514 electrometer). PHBV exhibits a negative electrification whereas C30B exhibits almost no electrification. When both components are mixed during more than 5 min, the mixture behaves like C30B, which is a clear indication that PHBV pellets are coated by C30B particles. This was confirmed by scanning electron microscopy (SEM) observations (Fig. 2b and c). These physical mixtures of PHBV pellets/2.5% C30B were then directly foamed by sc CO_2 assisted extrusion.

2.4. Foaming by sc CO_2 assisted extrusion

Fig. 3 shows the experimental set up. This process has been already used and described in previous works by Fages and co workers to produce foams of a pharmaceutical polymer named Eudragit [12] and foams of PHBV [39]. The single screw extruder (Rheoscam, Scamex, France) has a screw diameter of 30 mm and a length to diameter ratio (L/D) of 37. The screw is divided into four parts. The length to diameter ratio is of 20 for the first one, 7.5 for the two following ones and 2 for the last one. Between each part, a restriction ring has been fitted out in order to obtain a dynamic gastight, which prevents sc CO_2 from backflowing. This principle is classically implemented by using reverse screw elements in twin screw extruders [13]. The first conical part of the screw allows the transport, the melting and the plasticizing of polymers. Then, in the two following parts, the screw has a cylindrical geometry

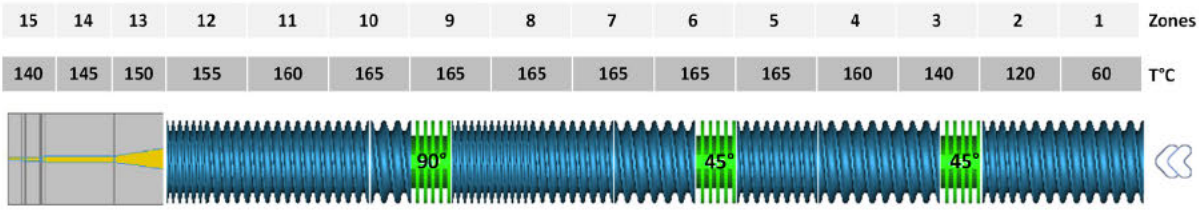

Fig. 1. Twin screw profile used for nanocomposites and masterbatches preparation.

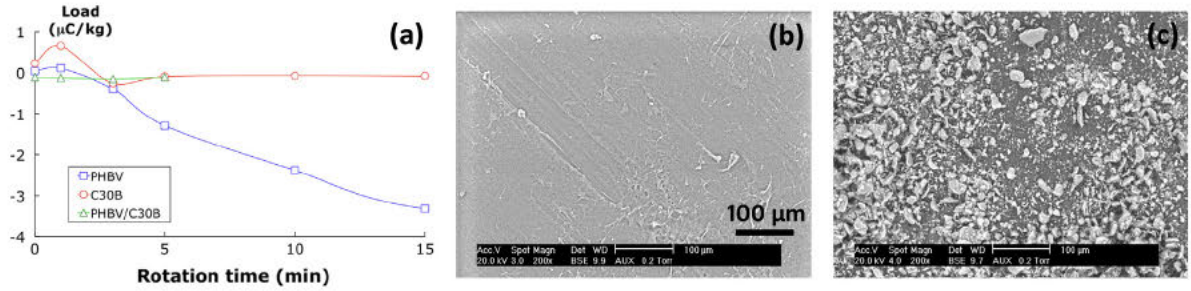

Fig. 2. Kinetics of triboelectrification (a) and SEM observations at the surface of (b) neat PHBV pellets and (c) PHBV/2.5% C30B (PM) physical mixtures.

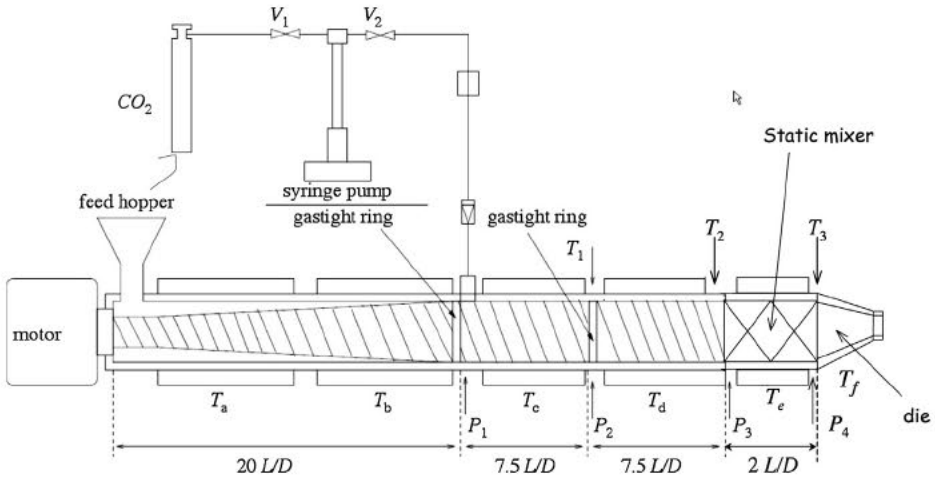

Fig. 3. Experimental device used for the foaming by sc CO_2 assisted single screw extrusion.

from the first gastight ring to the last part. The fourth part, which is removable, contains four static mixer elements with a diameter of 17 mm (SMB H 17/4, Sulzer, Switzerland). Three different cylindrical dies have been tested (Table 1).

The temperature inside the barrel is regulated at six locations: T_a and T_b before the sc CO_2 injection, T_c and T_d after the sc CO_2 injection, T_e in the static mixer and T_f in the die. For all experiments, T_a, T_b and T_c were fixed at 160 °C to ensure the melting of the PHBV matrix while limiting thermal degradation. The polymer temperature was then reduced at the exit of the die in order to favour foaming. T_d and T_e were fixed at 140 °C and T_f not higher than 140 °C. There are four pressure and three temperature sensors: P_1 after the sc CO_2 injector, P_2 and T_1 before the second gastight ring, P_3 and T_2 before the static mixer and P_4 and T_3 by the die. This allows measuring the temperature and the pressure of the polymer during the extrusion process.

Table 1
Dimensions of the dies of the single screw extruder.

Die	Length (mm)	Diameter (mm)
L5	5	0.5
L12	12	1
L20	20	1

CO_2 (N45, Air liquide, France) is pumped from a cylinder by a syringe pump (260D, ISCO, USA) and then introduced at constant volumetric flow rate. The pressure in the CO_2 pump is kept slightly higher than the pressure P_1. The sc CO_2 injector is positioned at a length to diameter ratio of 20 from the feed hopper. It corresponds to the beginning of the metering zone, that is to say the part where the

Table 2
Foaming experimental conditions.

Mixtures	Screw speed (rpm)	T_f (°C)	w_{CO2} (mass%)	Static mixer	Die
Neat PHBV	30	120 140	1.5	No	L20
Neat PHBV	30	140	0 4	No	L20
PHBV/2.5% C30B (PM)	40	140	0 3	Yes	L5
PHBV/2.5% C30B dil. 20% (EX)	55	140	0 4	Yes	L20

channel depth is constant and equal to 1.5 mm. The pres sure, the temperature and the volumetric sc CO_2 flow rate are measured within the syringe pump. sc CO_2 density, obtained with the equation of state established by Span and Wagner [40], is used to calculate mass flow rate and thus the sc CO_2 mass fraction w_{CO2}. Once steady state con ditions are reached with the chosen operating conditions, extrudates were collected and water cooled at ambient temperature. Several samples were collected during each experiment in order to check the homogeneity of the extrudates. Several CO_2 mass fractions were tested until the maximum CO_2 flow rate, which is reached when desta bilisation of the polymer flow occurs. Experimental condi tions chosen after preliminary trials are summarized in Table 2 and they are discussed in Section 3.2.2.

2.5. Residence time distribution determination

The residence time distribution (RTD) has already been measured in this extruder with several polymers to quan tify the influence on the melt flow behaviour of both the sta tic mixers and the sc CO_2 [41,42]. In order to obtain additional information about the quality of the mixing, a trial has been carried out to follow the C30B as a tracer into the PHBV flow by using the same method as described by Common et al. [42]. A small quantity of physical mixture, i.e. PHBV pellets coated with C30B (see Section 2.3), has been introduced in the hopper and detected by means of a Raman probe placed just before the die. No characteristic peak of the C30B has been detected in the Raman signals whatever the amount of C30B introduced. However, con trarily to the study by Common et al. [42] done with tita nium dioxide, the whole Raman signal has been displaced towards lower intensities according to C30B concentration. The variation in the intensity of the main polymer peak as a function of time in the presence of tracer was hence used for the RTD determination.

2.6. Rheological behaviour

The rheological properties of the extruded PHBV based nanocomposites were carried out in dynamic oscillation mode using a strain controlled rheometer ARES (TA Instru ment, USA) equipped with a parallel plate geometry. The upper and lower plates were 25 mm in diameter. The gap was progressively set to around 2 mm and a delay was applied to reach the equilibrium (zero normal force) before starting frequency sweeps. Frequency sweep tests were performed at 165 °C, as for the extrusion process, from 0.1 to 100 rad/s. The linear viscoelastic domain was checked for all mixtures and the minimum limit strain recorded, i.e. 0.6%, was used for all experiments. The measurements were done three times for each blend and were well repro ducible. For all mixtures, the thermal stability time at 165 °C was over 8 min and the frequency sweep test dura tion was less than 6 min.

2.7. Wide angle X ray diffraction (WAXD)

The wide angle X ray diffraction measurements were performed using an AXS D8 Advance diffractometer (Bru ker, Germany) equipped with a Cu cathode ($\lambda = 1.5405$ Å) and a Vantec detector. Measurements were performed in reflection mode on powdered extrudates in the range $2\theta = 1.5$ 63.5° with a step size of 0.007° and a step time of 24.5 s. The interlayer distance d_{001} of the C30B clays were determined from the (001) diffraction peak using Bragg's law, $\lambda = 2d \sin\theta$.

2.8. Differential Scanning Calorimetry (DSC) experiments

The crystallization of PHBV and PHBV/clays blends and foams was characterized with a Pyris Diamond DSC (Per kin Elmer, Germany) equipped with an Intracooler II using nitrogen as the purge gas. The temperature and heat flow were calibrated with indium. Samples of 10 15 mg were sealed in aluminium pans, and analyzed from 20 °C to 200 °C at a heating and cooling rate of 10 °C/min. Three samples per mixture were tested. The degree of crystallin ity X_c was determined according to Eq. (1):

$$X_c \quad (|\Delta H_m|)/(f_p \times |\Delta H_m^0|) \times 100 \qquad (1)$$

where ΔH_m (J/g) is the melting enthalpy of the PHBV matrix, f_p is the PHBV weight fraction in the sample and $\Delta H_m{}^0$ (J/g) is the melting enthalpy of a pure crystal and $\Delta H_m{}^0 =$ 146 J/g for PHB [43]. No values for PHBV with varying valerate amounts can be found in literature.

2.9. Porosity

Porosity ε is defined as the ratio of void volume to the total volume of the sample and can be calculated by Eq. (2):

$$\varepsilon \quad 1 \quad \rho_{app}/\rho_p \qquad (2)$$

where ρ_{app} is the apparent density calculated from the weight of the samples and their volumes evaluated by measuring their diameter and length with a vernier (Facom, France). Nine measurements per sample were made to ensure a good accuracy. ρ_p is the bulk polymer density, determined by helium pycnometry (Micromeri tics, AccuPYC 1330), which is about 1216 kg m ^{3}.

2.10. Scanning (SEM) and Transmission Electron (STEM) Microscopy observations

The structures of nanocomposites and masterbatches were observed with a Quanta 200 FEG (FEI Company, The Netherlands) scanning electron microscope equipped with an external STEM module allowing to observe thin samples in transmission mode. The acceleration voltage varied from 7 to 10 keV. Ultra thin specimens with a thickness of 70 nm were cut from the middle section of moulded specimens, perpendicular to the flow direction of the melt during the injection. The cut was performed under cryogenic conditions with an ultramicrotome using a diamond knife at 80 °C, and the specimens were deposited on Cu grids. It should be noticed that the PHBV is very sensitive to electron beam, which made focusing the beam difficult.

The surfaces of PHBV pellets and the fracture surfaces of foamed extrudates were observed using an Environmental Scanning Electron Microscope XL30 ESEM FEG (Philips, The Netherlands). The surfaces were sputter coated with gold to avoid any degradation during observation. On the basis of the images obtained, a mean diameter D_{cell} is determined and a cell density N_{cell} per volume unit of unfoamed sample were calculated according to Eq. (3) [29,24,32]:

$$N_{cell} \quad \frac{N^{3/2}}{A} \frac{\rho_p}{\rho_{app}} \tag{3}$$

where N is the number of cells on an SEM image, A the area of the image, ρ_{app} the apparent density of the foam and ρ_p the bulk polymer density.

3. Results and discussion

3.1. Characterization of the PHBV/C30B extruded mixtures

3.1.1. Structure of PHBV/C30B nanocomposites and masterbatches

The structure of the PHBV/C30B nanocomposites and masterbatches were investigated by two complementary methods, WAXD and STEM. The WAXD measurements allowed to determine the interlayer distance of the C30B clays within the PHBV matrix. The STEM gave a direct visualization of the clay dispersion within the matrix. Three dispersion states can be obtained with this type of clays: aggregated, intercalated and exfoliated [7]. The aggregated state is the initial shape of the clays and it can be observed when the clays are not or badly dispersed due to poor affinity with the matrix. The intercalation state results from the limited insertion of the polymer chains in the interlayer spacing of the clays. The exfoliated state is characterized by the insertion of the polymer chains in large quantity and the delamination of the clay layers, which leads to a nanostructured composite associated with significant changes in the matrix properties at low clay contents, typically from 2% to 3% w/w. The processing conditions and the physico chemical affinity between the clays and the polymer matrix are the main factors influencing the dispersion state.

WAXD patterns are presented in Fig. 4 for the PHBV, the PHBV/2.5% C30B (EX) nanocomposite, the PHBV/10% and 20% C30B (EX) masterbatches (Fig. 4a) and the PHBV/2.5% C30B dil. 10% and 20% (EX) nanocomposites (Fig. 4b). Neat PHBV shows a weak and broad diffraction peaks in the range $2\theta = 1.5$ 4°, whereas C30B clays exhibit a peak at $2\theta = 4.9°$, which corresponds to an interlayer distance of 18 Å. Two diffraction peaks are detected on the patterns of the PHBV/10% and 20% C30B (EX) masterbatches (Fig. 4a). The first peak at a d_{001} distance of about 17 18 Å corresponds to the initial interlayer distance of C30B, meaning that a part of the clays is still aggregated for PHBV/10% and 20% C30B (EX) masterbatches. This first peak at 17 18 Å is not visible anymore for PHBV/2.5% C30B (EX) suggesting that there is no remaining aggregates in the nanocomposite. The second peak observed at lower angles corresponds to a d_{001} distance of 38 Å, 36 Å, 34 Å for PHBV/C30B containing 2.5%, 10% and 20% w/w C30B, respectively. The strong increase of the d_{001} distance indicates an important intercalation of the polymer chains within the interlayer space of the clays. Similar results were found by Choi et al. [44] and Bordes et al. [45] for PHBV/2% and 3% C30B and PHBV/2.6% C30B, respectively, prepared by melt intercalation. The authors found interlayer distances of 36.8 Å and 38.5 Å for PHBV/2% and 3% C30B and PHBV/2.6% C30B, respectively. This indicates that the twin screw extrusion process used in this work allowed a good dispersion of the C30B clays. In particular, the intensity of the peak at 38 Å for the PHBV/2.5% C30B (EX) is weak suggesting a possible exfoliation of the clays. The peak intensity increases with clay content, which

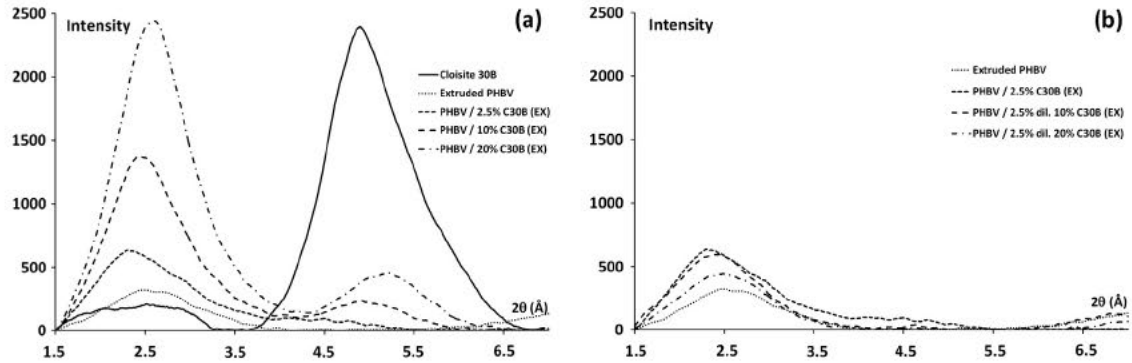

Fig. 4. WAXD patterns of (a) effect of C30B content: Cloisite 30B, extruded PHBV, PHBV/2.5% C30B (EX) nanocomposite and PHBV/10% and 20% C30B (EX) masterbatches, and (b) effect of the dilution: PHBV/2.5% C30B (EX) nanocomposite and PHBV/2.5% C30B dil. 10% and 20% (EX) nanocomposites.

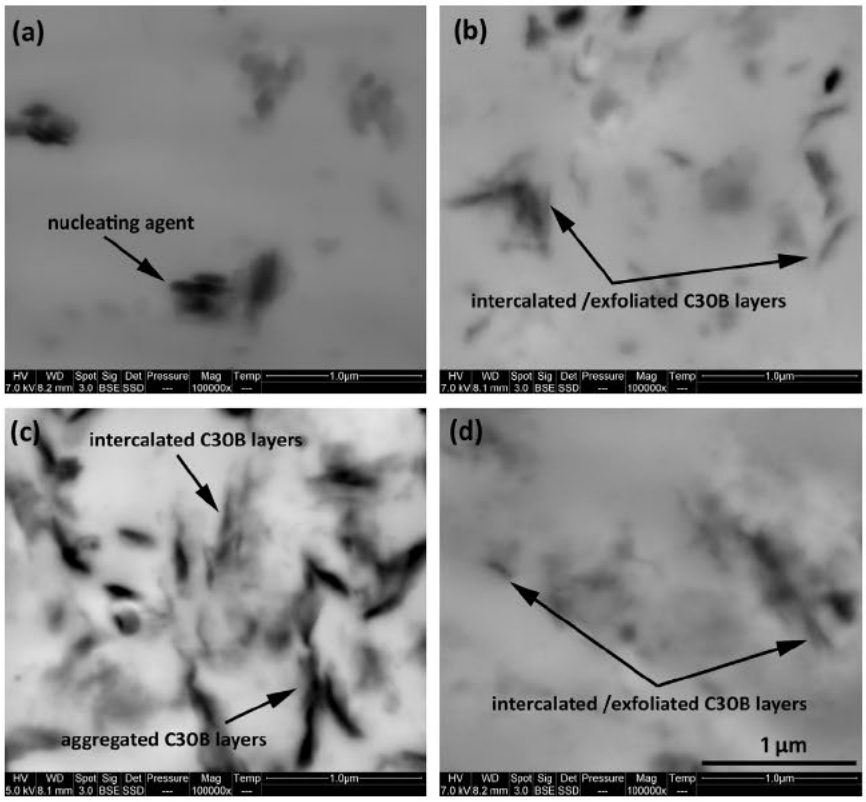

Fig. 5. STEM pictures (X 100000) of (a) extruded PHBV, (b) PHBV/2.5% C30B (EX) nanocomposite, (c) PHBV/20% C30B (EX) masterbatch, and (d) PHBV/2.5% C30B dil. 20% (EX) nanocomposite.

indicates an increase of the number and the size of the intercalated structures [45] for the PHBV/10% and 20% C30B (EX) masterbatches.

Masterbatches have been diluted to analyze the effect of the dilution on the dispersion of the clays. It is very interesting to observe that the WAXD patterns are very similar for the PHBV/2.5% C30B (EX) nanocomposite and the PHBV/2.5% C30B dil. 10% and 20% (EX) nanocomposites diluted from the masterbatches in the single screw injection press (Fig. 4b). The use of masterbatches to produce PHBV/2.5% C30B nanocomposites gives similar nanostructures while providing unprocessed and hence non degraded PHBV in the mixture. The good dispersion capacity of the clays is attributed to the good physico chemical interactions between PHBV and C30B that origi nates from strong hydrogen bonding between the ester carbonyl groups of PHBV and the hydroxyl groups in the interlayer space of C30B [44].

These results were confirmed by the STEM pictures (Fig. 5), on which aggregates and intercalated layered structures can be observed for PHBV/20% C30B (EX) (Fig. 5c), whereas mostly intercalated and possibly exfoli ated layered structures are observed for the PHBV/2.5% C30B (EX) (Fig. 5b) and the PHBV/2.5% C30B dil. 20% (EX) nanocomposites (Fig. 5d). Some black circular particles of boron nitride (as determined by energy dispersive X ray spectroscopy), i.e. the nucleating agent present in the PHBV, can also be observed (Fig. 5a).

3.1.2. Crystallization of PHBV/C30B nanocomposites and masterbatches

The effect of the clay content on the crystallization behaviour has been investigated by DSC. Fig. 6 presents the cooling and the second heating scans of the PHBV/ C30B nanocomposites and masterbatches. The cooling and second heating thermograms of PHBV are strongly modified by the addition of C30B. As reported in Table 3, the two melting peaks are shifted to lower temperatures (T_{m1} and T_{m2}) and the first peak becomes weaker with increasing C30B contents. The degree of crystallinity X_c as well as the crystallization temperature T_c are not affected by the addition of 2.5% C30B meaning that no significant nucleating effect occurs with the clays as was also recently reported by Carli et al. [46] for PHBV/C30B nanocompos ites. This should be attributed to the presence of boron nitride particles that already activates the nucleation of the commercial PHBV matrix used. For higher clays con tents 10% and 20% of C30B, a significant decrease of the degree of crystallinity X_c and the crystallization tempera ture T_c is measured. However, it is interesting to observe that the crystallization and melting behaviour of the PHBV/2.5% C30B dil. 20% (EX) nanocomposite is similar to those of PHBV/2.5% C30B (EX) nanocomposite suggest ing that the dilution of the PHBV/20% C30B (EX) master batch allow to recover the crystallization characteristics of the PHBV/2.5% C30B (EX). The masterbatch route thus appears has viable to prepare PHBV/clays nanocomposites.

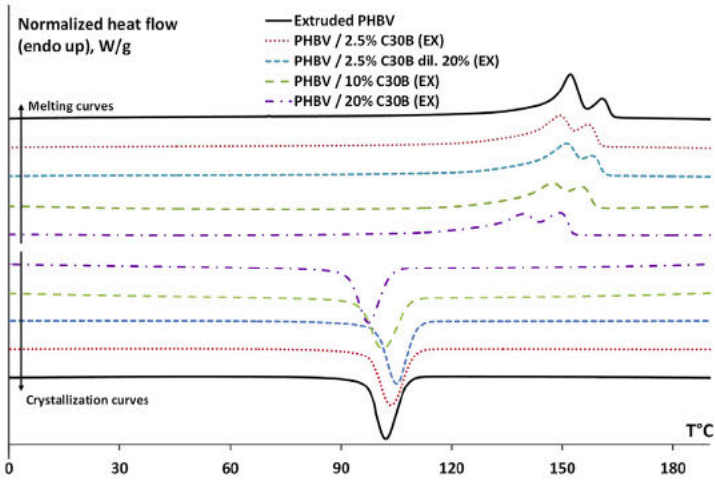

Fig. 6. Melting (second heating scan) and crystallization (cooling scan) curves of extruded PHBV and PHBV/C30B extruded mixtures.

Table 3
DSC data of melting (second heating scan) and crystallization (cooling scan) for neat PHBV and PHBV/C30B (EX) extruded mixtures.

Mixtures	T_{m1} (°C)	T_{m2} (°C)	T_c (°C)	ΔH_m (J/g)	X_c (%)
Extruded PHBV	154.3 ± 1.8	162.2 ± 1.1	104.4 ± 1.7	61.4 ± 0.7	42.0 ± 0.5
PHBV/2.5% C30B (EX)	150.7 ± 2.1	158.2 ± 1.8	103.2 ± 1.5	59.9 ± 1.9	42.0 ± 1.4
PHBV/2.5% C30B dil. 20% (EX)	151.8 ± 0.7	158.4 ± 0.3	105.0 ± 0.0	60.1 ± 0.6	42.1 ± 0.4
PHBV/10% C30B (EX)	148.4 ± 1.1	155.7 ± 0.7	101.2 ± 0.9	47.9 ± 2.8	36.0 ± 2.1
PHBV/20% C30B (EX)	141.2 ± 1.7	150.4 ± 1.0	98.7 ± 2.4	41.1 ± 3.6	35.4 ± 3.1

The presence of two melting peaks has already been reported for PHBV/C30B nanocomposites. Carli et al. [46] measured a decrease of the melting temperature associ ated with the appearance of a second melting peak and a broadening of the (1 1 0) and (1 0 1) diffraction peaks with the addition of C30B clays in the PHBV matrix. Bordes et al. [45] reported the presence of two melting peaks for both PHBV and PHBV/C30B nanocomposites, and an increased intensity of the first melting peak associated with a shift to lower temperature with increasing clay con tent. However, the temperature of the second melting tem perature did not change. In both studies, these observations were attributed to the formation of less per fect crystals with lower thermal stability due to the pres ence of the clays that affects the crystallization upon cooling. Besides, the presence [45] or the formation [46] of two melting peaks should be related to the recrystalliza tion phenomenon. As demonstrated by Gunaratne and Shanks [47] from step scan DSC experiments, the less per fect and first melted crystals can reorganize during heating to further melt at higher temperatures, giving a second melting peak. In this study, the fact that the two melting peaks and the crystallization peak are shifted to lower temperatures as well as the decrease of the degree of crys tallinity with high C30B contents indicates that an addi tional phenomenon occurred. The formation of less perfect crystals should also be affected by the degradation of the PHBV with the clays due to, (i) the presence of Al Lewis and Bronsted acid sites in the inorganic layers which catalyzes the hydrolysis of ester linkage [2,48 50], and (ii) the clay organomodifier and its potential decomposition products that also catalyse the PHBV degradation upon extrusion [6,10].

As shown above, the dilution of the PHBV/20% C30B (EX) masterbatch to 2.5% C30B allowed to recover the crys tallization characteristics of the PHBV/2.5% C30B (EX). The masterbatch route thus appears has viable to prepare PHBV/clays nanocomposites.

3.1.3. Rheological behaviour

The rheological behaviour of extruded PHBV and PHBV/ C30B nanocomposites compared to unprocessed PHBV confirmed the above hypothesis of PHBV degradation. As shown in Fig. 7, the zero shear rate viscosity of the extruded PHBV is strongly decreased after the extrusion process. It is divided by 4.7 as compared to the unpro cessed PHBV. This can be directly related to a decrease of the average molecular weight of the PHBV chains due to thermal degradation and shearing upon extrusion. An extensive decrease of the number and weight average molecular weights up to 37% and 52%, respectively, was also reported for extruded [3] and injected [4] PHBV con taining 8 9% w/w of HV. When adding 2.5% C30B, a strong shear thinning behaviour is observed at high frequencies. The rheological behaviour at high frequencies is known to be mainly determined by the properties of the polymer matrix with little influence of the clays. As shown in Fig. 7, the viscosity of PHBV/2.5% C30B (EX) is significantly decreased even if compared with extruded PHBV, high lighting the catalytic degradation effect of the clays on the PHBV matrix. Nevertheless, it should be mentioned that the C30B organomodifier was found to offer a good

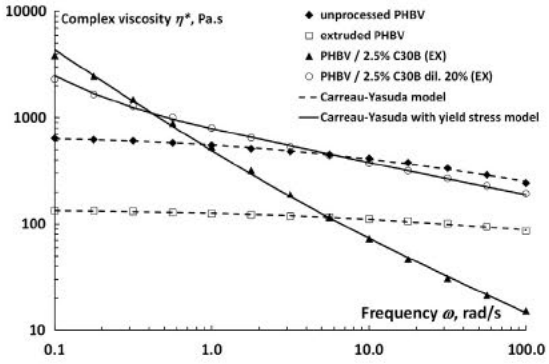

Fig. 7. Complex viscosity η versus frequency ω at 165 °C for unprocessed PHBV, extruded PHBV, PHBV/2.5% C30B (EX) and PHBV/2.5% C30B dil. 20% (EX).

compromise between the dispersion capacity of the clays and limited polymer degradation [6].

The rheological behaviour of nanocomposites at low frequencies is known to be mostly determined by the dispersion of the particles and their interactions. As shown in Fig. 7, a strong increase of the viscosity at low frequencies by 6 and 28.4 is observed for PHBV/2.5% C30B (EX) as compared to unprocessed and extruded PHBV, respectively. This phenomenon could be related to the formation of a percolated network of clays with a pseudo solid like behaviour at low frequencies characterized by a yield stress. This was firstly supported by several authors [51 53] for polystyrene/clay nanocomposites and recently also observed for polyester/clay systems such as poly (ε caprolactone)/clay nanocomposites [54] and PLA/PHBV/clay nanocomposites [33]. The better the dispersion, the highest will be the clays/matrix interactions and the viscosity at low frequencies. The rheological behaviour of such nanocomposite structures can be modelled by adding a yield stress parameter in the well known Carreau Yasuda model [55].

$$\eta^*(\omega) \quad \frac{\sigma_0}{\omega} + \eta_0[1 + (\lambda\omega)^a]^{(n-1)/a} \tag{4}$$

where η is the complex viscosity, ω is the frequency, σ_0 is the yield stress, η_0 is the zero shear viscosity, λ is a characteristic time, a is the Yasuda parameter, and n is the flow index reflecting shear thinning. Eq. (3) was successfully used for polypropylene/clays nanocomposites [56,57]. In this study, flow index n was determined from the slope of each $\eta(\omega)$ curve at high frequencies and yield stress from stress frequency dependence extrapolated to zero frequency. The model was thus reduced to three adjustable parameters (i.e. η_0, λ and a). Microsoft Solver© in Excel© was used to obtain the best fit with the experimental data (fits shown in Fig. 7). By this method, the yield stress, the zero shear viscosity, the relaxation time, and the flow index calculated for PHBV/2.5% C30B (EX) were 426 Pa, 133 Pa s, 0.1 s and 0.32, respectively.

When diluting the PHBV/20% C30B (EX) masterbatch to 2.5% C30B, it is interesting to observe that the viscosity of the unprocessed PHBV is almost recovered at high frequencies due to the input of unprocessed and hence non degraded PHBV in the mixture. Melt flow indexes and zero shear viscosities are 0.72 and 0.71, and 676 Pa s and 687 Pa s for unprocessed PHBV and PHBV/2.5% C30B dil. 20% (EX), respectively. The pseudo solid like behaviour at low frequencies is slightly less pronounced with a yield stress of 179 Pa, meaning that the quality of the dispersion could be a little reduced as compared to directly extruded PHBV/2.5% C30B (EX). This can be explained by the lower dispersive capacity of the single screw of the injection press used to investigate the dilution effect, as compared to the twin screw extruder. However, the WAXD (Fig. 4) and the STEM (Fig. 5) experiments showed that the nano structures for the PHBV/2.5% C30B (EX) and the PHBV/2.5% C30B dil. 20% (EX) were very similar.

This preliminary study on the structure, i.e. dispersion of the clays and crystallization behaviour, and the rheological behaviour of the PHBV/2.5% C30B (EX) nanocomposite and the one produced from the masterbatch, PHBV/2.5% C30B dil. 20% (EX), allowed to demonstrate that the dilution of the masterbatches to lower clay contents in a single screw apparatus is a good approach to prepare PHBV/C30B nanocomposites with good dispersion and limited degradation. The physico chemical affinity between the PHBV and the C30B clays is one of the main reasons for this good dispersion capacity. In the following, this dilution procedure has thus been used to prepare PHBV/2.5% C30B dil. 20% (EX) nanocomposite foams, i.e. PHBV/20% C30B (EX) masterbatch was diluted to 2.5% C30B with unprocessed PHBV during the sc CO_2 assisted single screw extrusion. The obtained foams are compared to PHBV/2.5% C30B (PM) foams directly produced from physical mixtures.

3.2. Processing and characterization of the PHBV/clays nanobiocomposite foams

3.2.1. RTD measurements

Fig. 8 shows RTD obtained for typical operating conditions used for pure PHBV foaming: no static mixer, screw rotation speed at 30 rpm, temperature at 140 °C and 150 °C (T_d and T_e being equal). Whatever the operating conditions, the Raman intensity variation remains at low levels, resulting in a noisy signal for the RTD. No significant influence of the temperature has been observed, partly due to the signal noise. The average residence time t_{moy} has

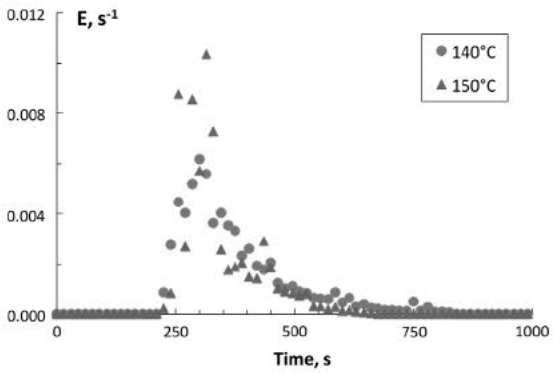

Fig. 8. RTD obtained without static mixer for a screw rotation speed at 30 rpm.

been found to be 345 ± 12 s, what is coherent with previous results [41,42]. Moreover, the onset time t_{app} (at which the beginning of the peak is detected) can be determined to calculate the ratio t_{app}/t_{moy}. This ratio is equal to 1 for a plug flow, to 0 in a perfectly mixed reactor and to about 0.75 for a single screw extruder [58]. In our case, it was evaluated at 0.7 ± 0.05, a value similar to the one measured for Polyamide 11 [42].

It has been already shown that the mixing is improved by the addition of a static mixer [42]. In this study, the addition of such a static mixer results in a too low Raman signal that can be no more detected. It confirms thus that the mixing of the C30B is improved although it is not possible to quantify this improvement.

3.2.2. Choice of the foaming conditions

The first trials with PHBV were carried out with the L12 die, but pressures obtained in the extruder were too low to allow sc CO_2 injection. In consequence, the L12 die was replaced by the L20 having a length of 20 mm to increase operating pressures. Screw speed can be varied from 30 to 80 rpm, but the lowest possible speed was selected to increase the residence time of the mixtures, and thus the mixing time. In the case of the extruded mixture, a decrease of operating pressures was observed with the addition of the clays. As discussed previously, rheological dynamic measurements showed that the presence of 2.5% of C30B can induce a viscosity decrease of the polymer. This phenomenon was particularly obvious at high shear rates, which usually occur during the extrusion. Thus, the screw speed was increased to 55 rpm for this mixture to increase operating pressures. In the case of the physical mixing, the pressure decrease was larger and the die L5 having a smaller diameter was used to increase the pressure and allow sc CO_2 injection.

Experimental conditions finally chosen are summarized in Table 2. There is thus clear evidence that the formulation of the PHBV induces a modification of the properties of the materials. This results in different behaviours in the extrusion process which requires a tailoring of the processing conditions.

3.2.3. Effect of the die temperature on the neat PHBV foams

The effect of the temperature has been already observed for several polymers [13]. In general, the porosity is a negative function of temperature because of the diffusivity of the blowing agent. Thereby the extensional rate and strain associated with cell growth increase with temperature, while melt viscosity and elasticity shows a reverse trend [59,60,24]. Moreover, the expansion ratio usually reaches a maximum according to the die temperature. Indeed, by freezing the surface of the extrudate at lower die temperatures, more gas remains in the foam to contribute to the volume expansion [59]. However, too low temperatures induce an increased stiffness of the frozen skin layer and hence a decrease of the volume expansion ratio.

Pressures and corresponding porosities as a function of the die temperature are summarized in Table 4 for the first produced foams. Pressure before the die significantly decreases with increasing temperature, due to the lowering of the viscosity. However, the porosity is rather independent of the die temperature.

Table 4
Pressures and corresponding porosities as a function of the die temperature for the neat PHBV foams.

T_f (°C)	P_4 (MPa)	ε (%)
120	23.3	48
130	22.2	46
140	19.2	47

As observed in Fig. 9, the porosity is inhomogeneous and badly dispersed in the PHBV extrudates. This could be attributed to a lack of mixing between the PHBV and the sc CO_2. Moreover, the crystallization of the PHBV upon cooling inside and at the exit of the die should also be responsible for this inhomogeneous porosity. The crystals in formation in the amorphous matrix indeed hamper the solubility and diffusion of sc CO_2 into the polymer. Consequently, the absorption and diffusion of the sc CO_2 takes place almost exclusively through the amorphous regions and the formed polymer/gas mixture is not uniform [13]. If the temperature is further decreased, clogging of the die occurs, especially with loaded polymer. Although increasing die temperature favour growth and coalescence of the pores, it seems that the properties of the polymer avoid a good control of the foaming by the temperature. A possible explanation is a rather low solubility of the CO_2 (which can be estimated by the maximal reachable CO_2 mass fraction) or a rapid decrease of its solubility due to the apparition of a crystalline phase, favoured by the CO_2 but in which the CO_2 is less soluble [61,24]. The maximal value of the CO_2 mass fraction was about 5%. Finally, a temperature T_f of 140 °C was found to be the best compromise between a good foaming capacity and a limited clogging, especially for the PHBV/2.5% C30B mixtures, to study the influence of the CO_2 mass fraction.

3.2.4. Effect of the sc CO_2 mass fraction on the neat PHBV and PHBV/2.5% C30B foams

The effect of the sc CO_2 mass fraction on the pressure P_4 is represented in Fig. 10a. Pressure at the die decreases up to 30% with increasing sc CO_2 mass fraction for all foams. This decrease is explained by the lower polymer viscosity induced by the plasticization effect of the sc CO_2.

The effect of the sc CO_2 mass fraction on the porosity ε is represented in Fig. 10b. In all cases, porosity decreases with increasing sc CO_2 mass fraction, which is rather astonishing since more sc CO_2 is theoretically available for foaming. This could be explained by a faster cooling of the extrudates, as sc CO_2 pressure drop is endothermic. The fast cooling thus increases the stiffness of the polymer which limits the growth of the cells and hence the expansion and the porosity. A part of the sc CO_2 could also be in excess [62] due to limited diffusion within the PHBV matrix or, as mentioned before, to the apparition of a crystalline phase favoured by the presence of the sc CO_2. This excess of sc CO_2 diffuses to the walls of the extruder and does not participate to cell nucleation. This also decreases

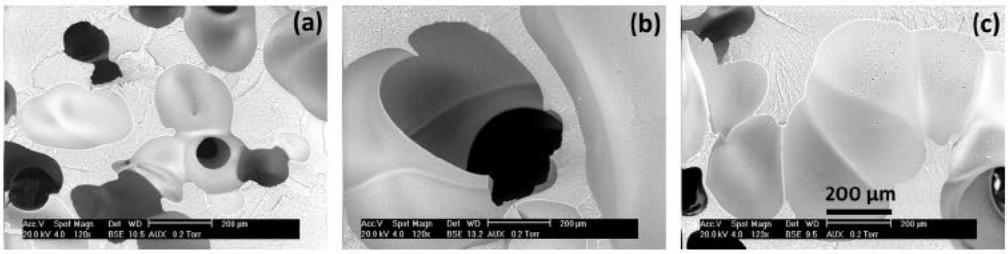

Fig. 9. SEM pictures for neat PHBV foams at various die temperature T_f, (a) 120 °C, (b) 130 °C, (c) 140 °C.

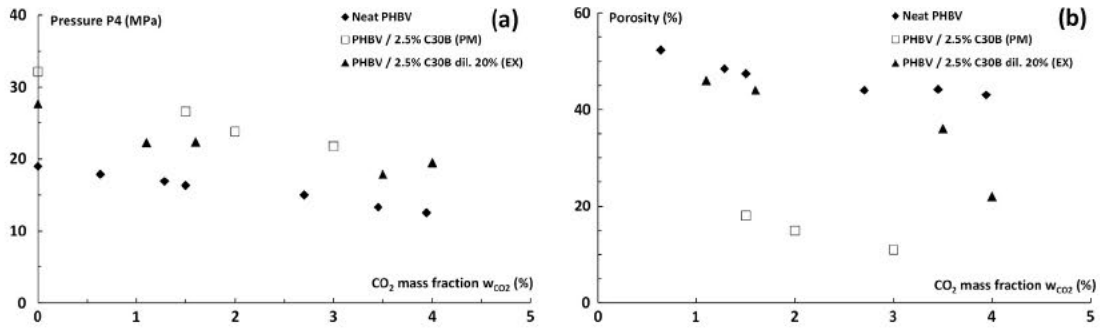

Fig. 10. Evolution of (a) the pressure P_4 and (b) the porosity ε as a function of the sc CO_2 mass fraction for foams of neat PHBV, PHBV/2.5% C30B dil. 20% (EX), PHBV/2.5% C30B (PM).

the processing pressures and temperatures, which in turn limits the expansion.

Even if it is difficult to compare the three formulations as they were obtained in different operating conditions, the clays does not seem to modify the evolution neither of the pressure nor of the porosity with the increase of sc CO_2 mass fraction. However, at high sc CO_2 mass fraction ($w_{CO2} > 3.5\%$), we can observe a significant decrease of the porosity for the extruded mixture, PHBV/2.5% C30B dil. 20% (EX) (Fig. 10b). This could be due to the presence of well dispersed clays which increases the cooling of the matrix and the crystallization kinetics, limiting the growth of the pores and the expansion of the foams. Indeed, clays are also known to improve the gas and fluid barrier properties of polymeric materials [63].

SEM pictures of the foam extrudates of neat PHBV and physical and extruded PHBV/2.5% C30B mixtures are represented in Fig. 11. When sc CO_2 mass fraction increases, pores become smaller, more numerous and regular. These observations are illustrated by the evolution of the cell density and the mean cell diameter in Fig. 12. It confirms that the presence of more sc CO_2 increases nucleation (higher cell density) but limits the growth and the coalescence of the pores (smaller mean diameters). The sc CO_2 mass fraction must thus be optimized to promote nucleation while keeping enough growth and expansion. Generally, the neat PHBV and PHBV/2.5% C30B foam structure dependency to sc CO_2 mass fraction can be summarized as follows:

(i) Low sc CO_2 mass fractions induce higher processing pressures and temperatures that promote extensive growth and higher porosity, but also less nucleation and poor homogeneity due to the coalescence of the pores.

(ii) High sc CO_2 mass fractions promote nucleation and homogeneity, but also induce lower processing pressures and temperatures and also increased cooling, that limit the growth and porosity due to the increased stiffness of the frozen polymer.

It can be also noticed that the neat PHBV and PHBV/2.5% C30B dil. 20% (EX) foams show similar results whereas the PHBV/2.5% C30B (PM) foam exhibits higher cell densities and smaller diameters, with however lower porosities. The use of a shorter and narrower die in the experiments of PHBV/2.5% C30B (PM) foam increases the pressure drop rate $\Delta P/\Delta t$, resulting in a higher nucleation, but increases also the cooling speed of the extrudates, thus hampering the growth of the foamy structure. It seems thus that the effect of the die is predominant in comparison to the heterogeneous nucleation due to presence of the dispersed clays.

3.2.5. Clays/foaming interrelationships and effect on the nanocomposite foams structure and crystallization

As shown in Fig. 11, the clay particles are inhomogeneously dispersed in the extrudates based on the PHBV/2.5% C30B (PM) physical mixtures. Several aggregates of 10 350 µm are observed whatever the sc CO_2 mass fraction. The effect of the sc CO_2 on the properties of the polymer matrix during single screw extrusion and the presence of static mixers were thus not sufficient to induce the intercalation of the polymer chains within the interlayer space of the C30B clays and their dispersion. The static mixers indeed enhance the distributive mixing of the sc CO_2 and the clays but only have little dispersive efficiency. Concerning the foam extrudates of PHBV/2.5% C30B dil. 20% (EX), a very good dispersion of the C30B is

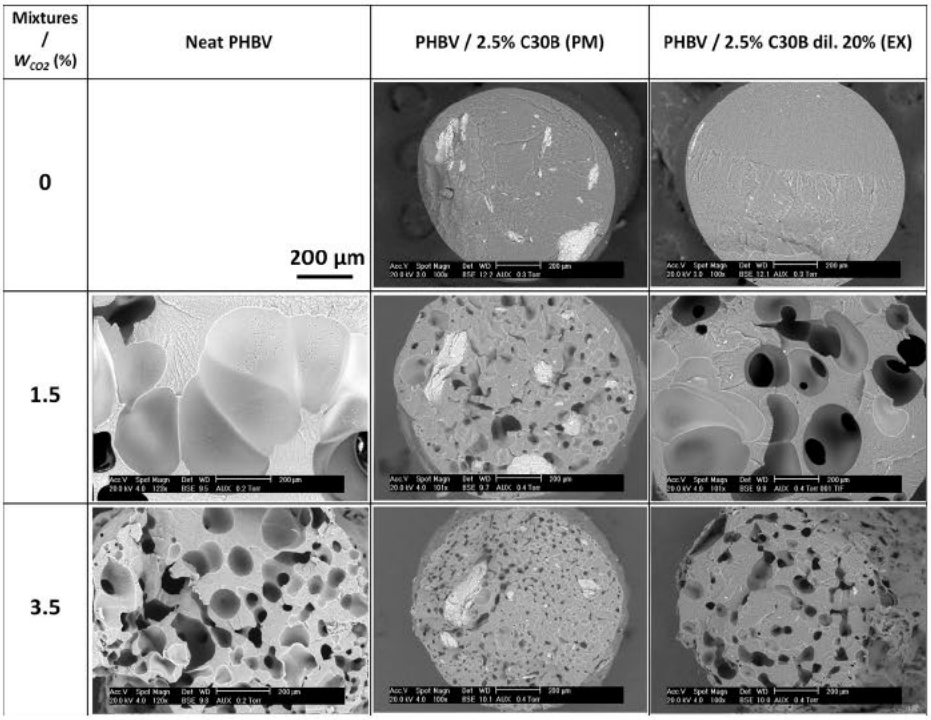

Fig. 11. SEM pictures of foam extrudates of neat PHBV, PHBV/2.5% C30B (PM) and PHBV/2.5% C30B dil. 20% (EX) foamed at different sc CO_2 mass fraction.

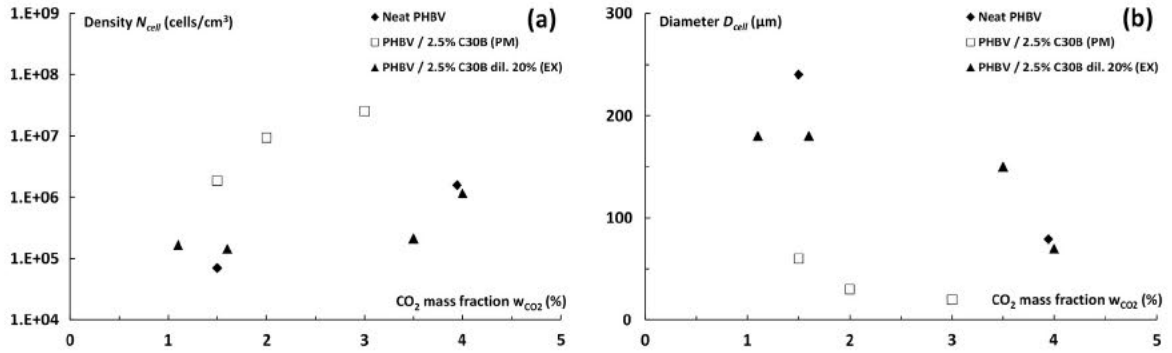

Fig. 12. Evolution of (a) the cell density N_{cell} and (b) the mean diameter D_{cell} as a function of the sc CO_2 mass fraction for foams of neat PHBV, PHBV/2.5% C30B (PM) and PHBV/2.5% C30B dil. 20% (EX).

observed with no visible aggregates (Fig. 11). This suggests that the prior preparation of a PHBV/20% C30B (EX) masterbatch and its further dilution to 2.5% C30B during the sc CO_2 assisted extrusion process is a necessary step to obtain good clay dispersion. As shown in Fig. 13, the position of the intercalation peaks at 36 38 Å remains unchanged after the foaming process whatever the sc CO_2 mass fraction. This suggests that, with the conditions and the materials used, sc CO_2 has no significant influence on the clay dispersion.

The dispersion capacity of the clays in PHBV processed in presence of sc CO_2 could be enhanced by improving their 'CO_2 philicity'. Indeed, the use of Cloisite 93A which presents 'CO_2 philic' acidic hydrogen on the surfactant was shown to significantly improve the clay dispersion in PDMS based nanocomposites prepared with sc CO_2 [16]. Specific clay modifications with surfactant as 2 methacryloyloxyethyl hexadecyldimethyl ammonium bromide (MHAB) were also shown to improve the interactions at the PS/clay interface, and hence the dispersion in PS/clays nanocomposite foams produced in autoclave with sc CO_2 [17]. Considering the poor thermal stability and the ease of hydrolysis of PHBV, modifications of the clay by surfactants must however be achieved with caution and in particular, acidic groups must be excluded. Bordes et al. [6] showed that the C30B organomodifier used in this study offers a good compromise between the dispersion capacity of the clays and limited PHBV degradation. In PHBV/clays

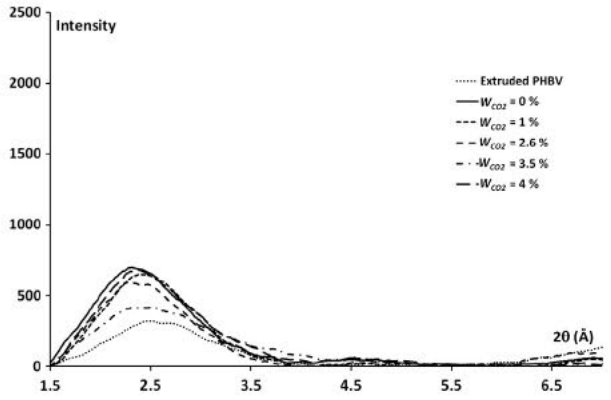

Fig. 13. WAXD patterns of extruded PHBV and PHBV/2.5% C30B dil. 20% (EX) nanocomposite foams obtained with increasing amount of sc CO_2.

Table 5
DSC data of neat PHBV and PHBV/2.5% C30B dil. 20% (EX) foamed at w_{CO2} = 1.5%.

Mixtures	T_{m1} (°C)	T_{m2} (°C)	T_c (°C)	ΔH_m (J/g)	X_c (%)
Neat PHBV foam	144.3	159.3	103.6	60.1	41.1
PHBV/2.5% C30B dil. 20% (EX) foam	146.2	160.2	106.2	58.4	40.0

systems foamed with sc CO_2, a possible improvement of the 'CO_2 philicity' and the dispersion capacity of the clays could be obtained by incorporating a surfactant bearing together hydroxyl groups to conserve a good affinity with PHBV and a 'CO_2 philic' carbonyl group. Polymer chains intercalation as well as sc CO_2 diffusion within the inter layer space of the clays would be enhanced.

A good dispersion of the clays has been reported to favour homogeneous nucleation and give porous structures with higher cell density [32,17,11]. As shown in Figs. 11 and 12b at low sc CO_2 mass fraction (w_{CO2} < 1.5%), extruded PHBV/2.5% C30B dil. 20% (EX) based foams indeed appear more homogeneous with rather smaller cell diameter and higher cell density as compared to neat PHBV foams, while showing equivalent porosity (see Fig. 10b). This has to be related with the presence of well dispersed clays within the walls of the pores which limits the coalescence and favours homogeneous nucleation. At high sc CO_2 mass fraction (w_{CO2} > 3.5%), the presence of the clays decreases significantly the porosity (Fig. 10b). As postulated above, the diffusion of the sc CO_2 within the PHBV matrix may be slightly hampered by the clays which increases the cooling of the matrix and the crystallization kinetics, limiting the growth of the pores and the expansion of the foams.

As shown in Tables 3 and 5, the degree of crystallinity remains unchanged after the sc CO_2 foaming process for both neat PHBV and PHBV/2.5% C30B dil. 20% (EX). However, the DSC spectra are significantly modified (Fig. 14). Indeed, the second melting peak T_{m2} becomes predominant and only a shoulder of the first melting peak T_{m1}, previously described (Fig. 6) and assigned to crystals of lower thermal stability, is observed for both neat PHBV and PHBV/2.5% C30B dil. 20% (EX) foams. This suggests that the sc CO_2 modifies the crystallization kinetics and mechanisms of the PHBV upon cooling at the end of the foaming process and induces the formation of more perfect crystals of higher thermal stability that melt at higher temperature. However, it has to be emphasized that the crystallization in the presence of dissolved CO_2 is complex because it implies contradictory phenomena as, for instance, it accelerates the cooling during depressurization while promoting higher mobility of the polymer chains. It can be noticed that a higher degree of crystallinity has already been obtained in the case of biopolyester PLA foams [22 24]. Besides, no significant influence was noticed on the crystallization of the foamed samples after melting in the DSC. Indeed, upon cooling in the DSC, melted neat PHBV and PHBV/2.5% C30B dil. 20% (EX) crystallise in the same temperature range and similar enthalpies as the samples that were not foamed (see Table 3). This indicates that sc CO_2 has only an effect on the crystallization upon the foaming process but no irreversible effect on the macromolecular structure of the polymer.

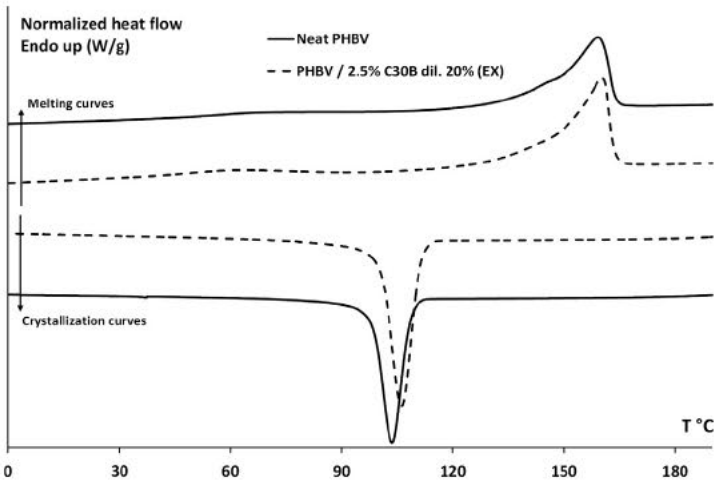

Fig. 14. Melting (first heating scan) and crystallization (cooling scan) curves of neat PHBV and PHBV/2.5% C30B dil. 20% (EX) foams (w_{CO2} = 1.5%) processed in the sc CO_2 assisted single screw extruder.

4. Conclusions

A continuous sc CO_2 assisted extrusion process has been implemented to prepare PHBV/organo clays nano biocomposite foams. The prior preparation of a master batch and its further dilution during the sc CO_2 assisted single screw extrusion process are necessary steps to obtain good clay dispersion and limited PHBV degradation. By controlling the sc CO_2 mass fraction in a narrow win dow, good clay dispersion appears to favour homogeneous nucleation while limiting the coalescence of the pores, and hence allows to obtain nano biocomposite foams with bet ter homogeneity and higher porosity up to 50%. Neverthe less, the crystallization of the PHBV upon the foaming process should hamper the diffusion of the sc CO_2 within the matrix and hence the nucleation and growth of the pores which limit the homogeneity and ultimate porosity of the foams. Further studies will thus focus on the foam ing of amorphous biopolyester by the continuous sc CO_2 assisted extrusion process developed in this study.

Acknowledgements

The authors thank the Carnot M.I.N.E.S Institute and the Nanomines group for financial support.

This paper is dedicated to the memory of our esteemed colleague Elisabeth Rodier who left us much too early.

References

[1] Khanna S, Srivastava AK, Khas H. Recent advances in microbial poly hydroxyalkanoates. Process Biochem 2005;40:2173 82.

[2] Bordes P, Pollet E, Avérous L. Nano biocomposites: biodegradable polyester/nanoclay systems. Prog Polym Sci 2009;34:125 55.

[3] Cabedo L, Plackett D, Giménez D, Lagaron JM. Studying the degradation of polyhydroxybutyrate covalerate during processing with clay based nanofillers. J Appl Polym Sci 2009;112:3669 76.

[4] Gogolewski S, Jovanovic M, Perren SM, Dillon JG, Hughes MK. The effect of melt processing on the degradation of selected polyhydroxyacids: polylactides, polyhydroxybutyrate, and polyhydroxybutyrate co valerates. Polym Degrad Stabil 1993;40:313 22.

[5] Ramkumar DHS, Bhattacharya M. Steady shear and dynamic properties of biodegradable polyesters. Polym Eng Sci 1998;38:1426 35.

[6] Bordes P, Hablot E, Pollet E, Avérous L. Effect of clay organomodifiers on degradation of polyhydroxyalkanoates. Polym Degrad Stabil 2009;94:789 96.

[7] Ray SS, Okamoto M. Polymer/layered silicate nanocomposites: a review from preparation to processing. Prog Polym Sci 2003;28:1539 641.

[8] Lertwimolnun W, Vergnes B. Influence of screw profile and extrusion conditions on the microstructure of polypropylene/organoclay nanocomposites. Polym Eng Sci 2007;47:2100 9.

[9] Treece MA, Zhang W, Moffitt RD, Oberhauser JP. Twin screw extrusion of polypropylene clay nanocomposites: influence of masterbatch processing, screw rotation mode, and sequence. Polym Eng Sci 2007;47:898 911.

[10] Hablot E, Bordes P, Pollet E, Avérous L. Thermal and thermomechanical degradation of PHB based multiphase systems. Polym Degrad Stabil 2008;93:413 21.

[11] Zeng C, Han X, Lee LJ, Koelling KW, Tomasko DL. Polymer clay nanocomposite foams prepared using carbon dioxide. Adv Mater 2003;15:1743 7.

[12] Nikitine C, Rodier E, Sauceau M, Letourneau J J, Fages J. Controlling the structure of a porous polymer by coupling supercritical CO_2 and single screw extrusion process. J Appl Polym Sci 2010;115:981 90.

[13] Sauceau M, Fages J, Common A, Nikitine C, Rodier E. New challenges in polymer foaming: a review of extrusion processes assisted by supercritical carbon dioxide. Prog Polym Sci 2011;36:749 66.

[14] Khosravi Darani K, Vasheghani Farahani E, Yamini Y, Bahramifar N. Solubility of poly(beta hydroxybutyrate) in supercritical carbon dioxide. J Chem Eng Data 2003;48:860 3.

[15] Cravo C, Duarte ARC, Duarte CMM. Solubility of carbon dioxide in a natural biodegradable polymer: determination of diffusion coefficients. J Supercrit Fluids 2007;40:194 9.

[16] Horsch S, Serhatkulu G, Gulari E, Kannan RM. Supercritical CO_2 dispersion of nano clays and clay/polymer nanocomposites. Polymer 2006;47:7485 96.

[17] Ngo TTV, Duchet Rumeau J, Whittaker AK, Gerard J F. Processing of nanocomposite foams in supercritical carbon dioxide. Part I: Effect of surfactant. Polymer 2010;51:3436 44.

[18] Tsimpliaraki A, Tsivintzelis I, Marras SI, Zuburtikudis I, Panayiotou C. The effect of surface chemistry and nanoclay loading on the microcellular structure of porous poly (D, L lactic acid) nanocomposites. J Supercrit Fluids 2011;57:278 87.

[19] Takahashi S, Hassler JC, KIran E. Melting behavior of biodegradable polyesters in carbon dioxide at high pressures. J Supercrit Fluids 2012;72:278 87.

[20] Jenkins MJ, Cao Y, Howell L, Leeke GA. Miscibility in blends of poly(3 hydroxybutyrate co 3 hydroxyvalerate) and poly(ε caprolactone) induced by melt blending in the presence of supercritical CO_2. Polymer 2007;48:6304 10.

[21] Reignier J, Gendron R, Champagne MF. Extrusion foaming of poly(lactic acid) blown with CO_2: toward 100% green material. Cell Polym 2007;26:83 115.

[22] Mihai M, Huneault MA, Favis BD, Li H. Extrusion foaming of semi crystalline PLA and PLA/thermoplastic starch blends. Macromol Biosci 2007;7:907 20.

[23] Mihai M, Huneault MA, Favis BD. Crystallinity development in cellular poly(lactic acid) in the presence of supercritical carbon dioxide. J Appl Polym Sci 2009;113:2920 32.

[24] Wang J, Zhu WL, Zhang HT, Park CB. Continuous processing of low density, microcellular poly(lactic acid) foams with controlled cell morphology and crystallinity. Chem Eng Sci 2012;75:390 9.

[25] Lee SM, Shim DC, Lee JW. Rheology of PP/clay hybrid produced by supercritical CO_2 assisted extrusion. Macromol Res 2008;16:6 14.

[26] Zhai W, Kuboki T, Wang L, Park CB. Cell structure evolution and the crystallization behavior of polypropylene/clay nanocomposites foams blown in continuous extrusion. Ind Eng Chem Res 2010;49:9834 45.

[27] Nofar M, Majithiya K, Kuboki T, Park CB. The foamability of low melt strength linear polypropylene with nanoclay and coupling agent. J Cell Plast 2012;48:271 87.

[28] Treece MA, Oberhauser JP. Processing of polypropylene clay nanocomposites: single screw extrusion with in line supercritical carbon dioxide feed versus twin screw extrusion. J Appl Polym Sci 2007;103:884 92.

[29] Han X, Zeng C, Lee JL, Koelling KM, Tomasko DL. Extrusion of polystyrene nanocomposite foams with supercritical CO_2. Polym Eng Sci 2003;43:1261 75.

[30] Nguyen QT, Baird DG. An improved technique for exfoliating and dispersing nanoclay particles into polymer matrices using super critical carbon dioxide. Polymer 2007;48:6923 33.

[31] Liu W, Wang XD, Li HQ, Du ZJ, Zhang C. Study on rheological and extrusion foaming behaviors of chain extended poly (lactic acid)/ clay nanocomposites. J Cell Plast 2013;49:535 54.

[32] Keshtkar M, Nofar M, Park CB, Carreau PJ. Extruded PLA/clay nanocomposite foams blown with supercritical CO_2. Polymer 2014;55:4077 90.

[33] Zhao H, Cui Z, Wang X, Turng L S, Peng X. Processing and characterization of solid and microcellular poly(lactic acid)/ polyhydroxybutyrate valerate (PLA/PHBV) blends and PLA/PHBV/ clay nanocomposites. Compos Part B Eng 2013;51:79 91.

[34] Zhao H, Cui Z, Sun X, Turng L S, Peng X. Morphology and properties of injection molded solid and microcellular polylactic acid/ polyhydroxybutyrate valerate (PLA/PHBV) blends. Ind Eng Chem Res 2013;52:2569 81.

[35] Javadi A, Srithep Y, Clemons CC, Turng LS, Gong SQ. Processing of poly(hydroxybutyrate co hydroxyvalerate) based bionanocomposite foams using supercritical fluids. J Mater Res 2012;27:1506 17.

[36] Qian J, Zhu L, Zhang J, Roberts SW. Comparison of different nucleating agents on crystallization of poly(3 hydroxybutyrate co 3 hydroxyvalerates). J Polym Sci Pol Phys 2007;45:1564 77.

[37] Singh S, Mohanty AK, Sugie T, Takai Y, Hamada H. Renewable resource based biocomposites from natural fiber and polyhydroxyburate co valerate(PHBV) bioplastic. Compos Part A Appl Sci Manuf 2008;39:875 86

[38] Zhang J, McCarthy S, Whitehouse R. Reverse temperature injection molding of Biopol™ and effect on its properties. J Appl Polym Sci 2004;94:483 91.
[39] Kamar K, Sauceau M, Rodier E, Fages J. Biopolymer Foam Production using a (SC CO_2) assisted extrusion process. In: 9th International symposium on supercritical fluids, Arcachon (France). <http://www.isasf.net/meetings/proceedings.html>; 2009.
[40] Span R, Wagner W. A new equation of state for carbon dioxide covering the fluid region from the triple point temperature to 1100 K at pressures up to 800 MPa. J Phys Chem Ref Data 1996;25:1509 96.
[41] Nikitine C, Rodier E, Sauceau M, Fages J. Residence time distribution of a pharmaceutical grade polymer/supercritical CO_2 melt in a single screw extrusion process. Chem Eng Res Des 2009;87:809 16.
[42] Common C, Rodier E, Sauceau M, Fages J. Flow and mixing efficiency characterisation in a CO_2 assisted single screw extrusion process by residence time distribution using Raman spectroscopy. Chem Eng Res Des 2014;92:1210 8.
[43] Barham PJ, Keller A, Otun EL, Holmes PA. Crystallization and morphology of a bacterial thermoplastic: poly 3 hydroxybutyrate. J Mater Sci 1984;19:2781 94.
[44] Choi WM, Kim TW, Park OO, Chang YK, Lee JW. Preparation and characterization of poly(hydroxybutyrate co hydroxyvalerate) organoclay nanocomposites. J Appl Polym Sci 2003;90:525 9.
[45] Bordes P, Pollet E, Avérous L. Structure and properties of PHA/clay nano biocomposites prepared by melt intercalation. Macromol Chem Phys 2008;209:1473 84.
[46] Carli LN, Crespo JS, Mauler RS. PHBV nano composites based on organomodified montmorillonite and halloysite: the effect of clay type on the morphology and thermal and mechanical properties. Compos Part A 2011;42:1601 8.
[47] Gunaratne LMWK, Shanks RA. Multiple melting behaviour of poly(3 hydroxybutyrate co hydroxyvalerate) using step scan DSC. Eur Polym J 2005;41:2980 8.
[48] Maiti P, Batt CA, Giannelis EP. New biodegradable polyhydroxybutyrate/layered silicate nanocomposites. Biomacromolecules 2007;8:3393 400.
[49] Pandey JK, Kumar AP, Misra M, Mohanty AK, Drzal LT, Singh RP. Recent advances in biodegradable nanocomposites. J Nanosci Nanotechnol 2005;5:497 526.
[50] Xie W, Gao Z, Pan W P, Hunter D, Singh A, Vaia R. Thermal degradation chemistry of alkyl quaternary ammonium montmorillonite. Chem Mater 2001;13:2979 90.
[51] Hoffmann B, Dietrich C, Thomann R, Friedrich C, Mülhaupt R. Morphology and rheology of polystyrene nanocomposites based upon organoclay. Macromol Rapid Commun 2000;21:57 61.
[52] Ren J, Silva AS, Krishnamoorti R. Linear viscoelasticity of disordered polystyrene–polyisoprene block copolymer based layered silicate nanocomposites. Macromolecules 2000;33:3739 46.
[53] Xu L, Reeder S, Thopasridharan M, Ren J, Shipp DA, Krishnamoorti R. Structure and melt rheology of polystyrene based layered silicate nanocomposites. Nanotechnology 2005;16:S514 21.
[54] Labidi S, Azema N, Perrin D, Lopez Cuesta JM. Organo modified montmorillonite/poly(epsilon caprolactone) nanocomposites prepared by melt intercalation in a twin screw extruder. Polym Degrad Stabil 2010;95:382 8.
[55] Berzin F, Vergnes B, Delamare L. Rheological behavior of controlled rheology polypropylenes obtained by peroxide promoted degradation during extrusion: comparison between homopolymer and copolymer. J Appl Polym Sci 2001;80:1243 52.
[56] Lertwimolnun W, Vergnes B. Influence of compatibilizer and processing conditions on the dispersion of nanoclay in a polypropylene matrix. Polymer 2005;46:3462 71.
[57] Lertwimolnun W, Vergnes B. Effect of processing conditions on the formation of polypropylene/organoclay nanocomposites in a twin screw extruder. Polym Eng Sci 2006;46:314 23.
[58] Thakur R, Vial C, Nigam K, Nauman E, Djelveh G. Static mixers in the process industries a review. Chem Eng Res Des 2003;81:787 826.
[59] Park CB, Behravesh AH, Venter RD. Low density microcellular foam processing in extrusion using CO_2. Polym Eng Sci 1998;38:1812 23.
[60] Sauceau M, Nikitine C, Rodier E, Fages J. Effect of supercritical carbon dioxide on polystyrene extrusion. J Supercrit Fluids 2007;43:367 73.
[61] Doroudiani S, Park CB, Kortschot MT. Effect of the crystallinity and morphology on the microcellular foam structure of semicrystallines polymer. Polym Eng Sci 1996;36:2645 62.
[62] Han X, Koelling KM, Tomasko DL, Lee JL. Continuous microcellular polystyrene foam extrusion with supercritical CO_2. Polym Eng Sci 2002;42:2094 106.
[63] Ray SS, Bousmina M. Biodegradable polymers and their layered silicate nanocomposites: in greening the 21st century materials world. Prog Mater Sci 2005;50:962 1079